Published June 1, 1993

Kinesin Follows the Microtubule's Protofilament Axis

Sanghamitra Ray, Edgar Meyhöfer, Ronald A. Milligan,* and Jonathon Howard

Department of Physiology and Biophysics SJ-40, University of Washington, Seattle, Washington 98195; * Department of Cell Biology, Scripps Research Institute, La Jolla, California 92037

Abstract. We tested the hypothesis that kinesin moves parallel to the microtubule's protofilament axis. We polymerized microtubules with protofilaments that ran either parallel to the microtubule's long axis or that ran along shallow helical paths around the cylindrical surface of the microtubule. When gliding across a kinesin-coated surface, the former microtubules did not rotate. The latter microtubules, those with supertwisted protofilaments, did rotate; the pitch and handedness of the rotation accorded with the supertwist measured by electron cryo-microscopy. The results show that kinesin follows a path parallel to the protofilaments with high fidelity. This implies that the distance between consecutive kinesin-binding sites along the microtubule must be an integral multiple of 4.1 nm, the tubulin monomer spacing along the protofilament, or a multiple of 8.2 nm, the dimer spacing.

MICROTUBULES form one component of the cytoskeleton of eukaryotic cells: they serve a structural role that is thought to help define the morphology of the cell, and they serve as tracks for intracellular motor proteins such as kinesin and dynein which transport organelles from one part of the cell to another.

The building blocks of a microtubule are dimers of the homologous α and β tubulin subunits. While the mechanism of polymerization of a microtubule from these heterodimers is not understood (Mandelkow and Mandelkow, 1990), the general structure of the microtubule is known. The dimers are associated in a head-to-tail fashion to form a protofilament whose axis roughly parallels that of the microtubule. Several protofilaments are then joined laterally to form a sheet which will define the wall of the microtubule. Closure of this sheet then gives rise to the hollow cylinder which is the microtubule. While most microtubules in vivo contain 13 protofilaments, microtubules containing as few as eight and as many as 19 have been observed in vivo and in vitro (for examples see Chrétien and Wade, 1991; Kikuchi et al., 1991; Böhm et al., 1990; Andreu et al., 1992). This heterogeneity of microtubule structure is the key to the work reported in this paper.

We have asked the question: along what path does the motor protein kinesin move? Does kinesin step from monomer to monomer (or dimer to dimer) along one protofilament, as suggested by some experiments (Vale and Toyoshima, 1988; Gelles et al., 1988; Kamimura and Mandelkow, 1992; and see Discussion)? Does kinesin take a more circuitous route moving systematically from protofilament to protofilament across the microtubule's surface lattice? Or does kinesin perhaps take a more unpredictable path, switching randomly between protofilaments?

To determine the path along which kinesin moves across the surface lattice of a microtubule, we have exploited the heterogeneity of microtubule structure alluded to above. In microtubules with 13 protofilaments (13 mers), the protofilaments are paraxial: the protofilament axis and the microtubule's long axis are parallel (Amos and Klug, 1974). In this way, the 0.946-nm longitudinal offset between monomers of neighboring protofilaments permits the formation of a three-start helix of the monomers: the accumulated circumferential offset of 13 × 0.946 nm exactly equals the length of three monomers (3 × 4.1 nm). However, when the protofilament number differs from 13, the accumulated offset is no longer integrally related to the subunit distance. In order that the protofilament sheet can close to form a microtubule, one (or both) of two structural alterations must take place: either the subunits deform under shear of the lattice so that the longitudinal offset is changed, or the protofilament sheet rotates so that the protofilaments no longer run parallel to the long axis of the microtubule. There is strong structural support for the latter type of alteration of the lattice structure which forms the basis for the lattice-rotation model (Langford, 1980; Wade et al., 1990*a*,*b*). If the protofilaments are not paraxial but instead "supertwist" around this axis, then a transmission electron micrograph of a non-13 mer whose longitudinal axis lies in the focal plane should show a periodic structure corresponding to the moiré pattern formed from the superposition of the front and back surfaces of the microtubule lattice. Such a moiré pattern was first observed using negative stain by Langford (1980). The better structural preservation afforded by electron cryo-microscopy (Adrian et al., 1984; Milligan et al., 1984) of hydrated, unstained microtubules allowed Wade et al. (1990*a*,*b*) to distinguish three classes of microtubules based on their diameters and moiré patterns;

Published June 1, 1993

cross-sections of the same population of microtubules indicated that the three classes corresponded to 13, 14, and 15 mers. The assignment of a protofilament number to a particular moiré pattern was confirmed for 14 mers (Chrétien and Wade, 1991) and for 12 mers (Andreu et al., 1992) by comparing the statistical distributions of protofilament numbers counted from thin cross-sections with the statistical distributions of the moiré patterns. Furthermore, Chrétien and Wade (1991) showed that the periods of the moiré patterns of the 12, 14, and 15 mers were in quantitative agreement with the lattice-rotation model, implying that the accommodation of one less and one or two more protofilaments is primarily attained by lattice rotation. The lattice-rotation model predicts that a 12-protofilament microtubule has a right-handed supertwist pitch of 3 to 4 μm and a 14-protofilament microtubule has a left-handed supertwist pitch of $\sim$6 μm. This prediction of the handedness of the supertwist by the lattice-rotation model has its origin in the assumed left-handedness of the three-start monomer helix of the 13-protofilament microtubule lattice (Amos and Klug, 1974).

These considerations of microtubule structure lead to a particularly simple test of the hypothesis that kinesin moves along a path parallel to the protofilaments: if this hypothesis is correct then we expect that in the microtubule-gliding in vitro motility assay, where kinesin is adsorbed to a surface and microtubules are observed to be moved across the surface in the presence of ATP, 13 mers should not rotate, whereas non-13 mers should rotate with the period and handedness of the supertwist (see Fig. 1). In this work, we tested these predictions.

Materials and Methods

Purification of Tubulin and Kinesin

Tubulin was purified to >95% homogeneity from bovine brain by two and a half cycles of depolymerization and polymerization, followed by phosphocellulose (ion exchange) chromatography to remove microtubule-associated proteins (Weingarten et al., 1974). The purified tubulin was then cycled again to remove any denatured protein and to exchange buffers if required (Hyman et al., 1991). Some tubulin was modified with X-rhodamine succinimidyl ester (Molecular Probes Inc., Eugene, OR) using the protocol of Hyman et al. (1991). Kinesin was purified from bovine brain using a method similar to that described by Wagner et al. (1991) except that endogenous microtubules were used for the initial affinity step (preparation developed by Fady Malik, University of California, San Francisco, CA). Kinesin was purified to $\sim$90% homogeneity with the main contaminant being tubulin.

Microtubule Assembly

The following buffers were used for microtubule polymerization at 37°C: Pipes buffer (80 mM Pipes, pH 6.8, with KOH; 1 mM $MgCl_2$; 1 mM EGTA, also called BRB80 in the literature), MES buffer (100 mM MES, pH 6.5, with HCl; 1 mM $MgCl_2$; 1 mM EGTA) and phosphate buffer (10 mM sodium phosphate, pH 7). In general, identical procedures were used to prepare microtubules used for EM and for the in vitro motility assays. The only major difference was dictated by two technical limitations of electron cryo-microscopy: first, the EM required high concentrations of microtubules and so an additional, final centrifugation step (TL 100; Beckman Instruments, Palo Alto, CA) was often necessary, and second, because the contrast in the EM images was reduced in high glycerol solutions an additional centrifugation and resuspension step was necessary.

Microtubule Assembly from Axoneme Doublets. Salt-washed axonemes and doublets were prepared from the sperm of the sea urchin *Strongylocentrotus purpuratus* (Gibbons, 1982). These were further purified by floating 10 ml of 0.35 mg/ml protein on a 10 ml 50% glycerol-Pipes buffer cushion and spinning for 1.5 h at 100,000 *g* in a rotor (F-28/26; Sorvall Instruments, Newton, CT). The pellet was washed with and resuspended in MES buffer to a concentration of 4 mg/ml total protein (Bradford, 1976). Before incubation with tubulin, 12 ml of the doublets were spun for 7 min at 19,000 *g* in a rotor (TMA-11; Tomy Tech USA, Inc., Palo Alto, CA) to remove aggregated doublets. 0.2 mg/ml of rhodamine-tubulin, 0.2 mg/ml tubulin, 1 mM GTP, 4 mM $MgCl_2$, and 10 μl of doublets were incubated in MES buffer. The total volume was 25 μl and after 100 min, 5 μl were diluted into 95 μl of 10 μM taxol in MES buffer and used for motility assays. The following changes were made for the cryo-EM: the total volume of microtubule polymerization solution was increased to 500 μl (the same final concentrations as above) and after incubation microtubules were centrifuged for 5 min at 70,000 rpm in a TLA 100.3 rotor and the pellet was resuspended in 10 μl of MES buffer.

Microtubule Assembly in Pipes-Glycerol and Pipes-seeded Microtubules. In a volume of 25 μl or 100 μl, 2.4 mg/ml rhodamine-tubulin, 1 mM GTP, 4 mM $MgCl_2$, and 36% glycerol were incubated in Pipes buffer for 15–20 min. These are called Pipes-glycerol microtubules. 1.3 μl of this mixture served as seeds when added to a second mixture, also in a volume of 25 or 100 μl and containing 2.2 mg/ml of tubulin, 1.6 mg/ml of rhodamine-tubulin, 1 mM GTP, 4 mM $MgCl_2$. After 30 min, 2 μl of this mixture was diluted into 98 μl of 10 μM taxol in Pipes buffer (prewarmed to 37°C) for motility assays. These are called Pipes-seeded microtubules. For cryo-EM, the microtubules were concentrated tenfold by centrifugation.

Microtubule Assembly in Pipes-DMSO. The procedure for Pipes-glycerol was modified: 5% DMSO was used instead of glycerol. For cryo-EM, 1.3 mg/ml rhodamine tubulin, 1.3 mg/ml tubulin, 4 mM $MgCl_2$, 1 mM GTP, and 5% DMSO were incubated in Pipes buffer for 20 min. For cryo-EM, the microtubules were concentrated tenfold by centrifugation.

Microtubule Assembly in Pipes. 2.5 mg/ml rhodamine-labeled tubulin, 2.5 mg/ml tubulin, 4 mM $MgCl_2$, and 1 mM GTP were incubated for 30 min in Pipes buffer. For cryo-EM, the microtubules were concentrated tenfold by centrifugation.

Microtubule Assembly in MES-Glycerol. The incubation was the same as Pipes-seeded except MES buffer was used. For cryo-EM, 3.5 mg/ml tubulin, 4 mM $MgCl_2$, 1 mM GTP, and 36% glycerol were incubated in MES buffer for 20 min, and then the microtubules were concentrated 2.5-fold by centrifugation.

Microtubule Assembly in MES-DMSO. 5.0 mg/ml tubulin, 4.0 mM $MgCl_2$, 1 mM GTP, and 5% DMSO were incubated in MES buffer for 20 min.

Microtubule Assembly in Phosphate-buffered taxol. 0.2 mg/ml rhodamine-tubulin, 1 mM GTP, 6 mM $MgCl_2$, and 2 μM taxol were incubated in phosphate buffer (pH 7) for over 3 h in a total volume of 250 μl. A tenfold dilution in Pipes buffer with 10 μM taxol was used for motility assays. For cryo-EM, 0.5 mg/ml rhodamine-tubulin, 1 mM GTP, 6 mM $MgCl_2$, and 5 μM taxol were incubated in phosphate buffer (pH 7) for 25 min in a total volume of 1 ml. Microtubules were concentrated by centrifugation to 25 μl.

Electron Cryo-microscopy

Vitrified preparations of microtubules grown under various assembly conditions were obtained by pipetting a 5-μl aliquot onto a glow discharged, holey-carbon-coated grid (1–3 μm). Depolymerization of microtubules was avoided by gently blowing saturated, humid air warmed to 37°C over the grid using an apparatus similar to that described by Chrétien et al. (1992). This was necessary because microtubules used for structural analysis were not taxol stabilized so that the possible confusion of the structure of the microtubules under study with those polymerized by addition of taxol was avoided. The grid was then blotted with prewarmed filter paper and the remaining solution of microtubules was rapidly frozen by plunging it into liquid ethane by means of a guillotine device. Specimens obtained in this manner were stored in liquid nitrogen, and then transferred to an electron microscope (CM12; Philips, Chesire, CT) equipped with a Gatan cryostage and anticontaminator. Grids were initially surveyed at low magnification. Images of the moiré patterns of vitrified microtubules were recorded at a magnification of 28,000× on SO 163 film (Eastman Kodak; Rochester, NY) using a low radiation dose (up to 10 $e^-/Å^2$). To increase the image contrast pictures were taken over holes in the carbon film and defocused by $\sim$2 μm.

Measurement of Microtubule Diameter and Moiré Periods

Morphological measurements were made on prints of magnification 70,000.

Published June 1, 1993

The diameter of a microtubule was defined by the way it was measured: the distance between the centers of the dark boundaries of the image was measured under a 25× dissection microscope at five positions along the microtubule and averaged. The moiré period was the distance over which the pattern repeated. Each repeat distance includes two fuzzy regions: this is also true for microtubules with an odd number of protofilaments (11 and 15) where the number of striations is the same on each side of the fuzzy region, but the off-centered patterns alternate from side-to-side (see Fig. 2).

Moiré Periods and Supertwist Pitches Predicted by the Lattice-Rotation Model

The hypothesis underlying the lattice-rotation model is that the local geometry of the protein lattice is independent of the number of protofilaments: that is the angle between the axis defined by the protofilament numbers and the axis defined by the three-start monomer helix remains unchanged with a change in protofilament number. The accommodation of different protofilaments is accomplished by a rotation of the whole lattice (Wade et al., 1990*a*,*b*; Chrétien and Wade, 1991). The concept is easily demonstrated using a sheet of paper on which the protofilaments have been drawn: if 13 protofilaments form a three-start helix then the mismatch introduced by a change in protofilament number can be compensated for by a rotation of the paper. This introduces a supertwist but clearly does not alter the local geometry because a sheet of paper cannot be sheared.

For a microtubule with n protofilaments forming an s-start helix in the monomers, the supertwist pitch, P, is

$$P = \frac{n_0 n^2 \delta^2}{z(n_0 s - s_0 n + \epsilon)}$$

where $n_0 = 13$ and $s_0 = 3$ are the canonical number of protofilaments and starts, $z = 4.1$ nm is the intermonomer distance along the protofilament, and $\delta = 5.15$ nm is the center-to-center distance between protofilaments (Chrétien and Wade, 1991). The number of starts, s, is an integer which corresponds to the number of the shortest-pitched monomer-helices that make up the microtubule. The period of the moiré pattern is P/n and the angle θ between the protofilament and microtubule axes is given by $\tan\theta = n\delta/P$. ϵ is a residual supertwist parameter whose value is zero if the protofilaments of a 13-protofilament microtubule run exactly parallel to the microtubule's long axis. $\epsilon = 0.574$, corresponding to a shallow supertwist of pitch 24.8 μm for a 13-protofilament microtubule, gives a somewhat better fit to the structural data. We checked this formula by computer simulations of the supertwist: the coordinates of the monomers were calculated according to the lattice rotation model and then the monomers were projected onto the plane to produce the moiré patterns shown in Fig. 2. The periods of the computer-generated patterns agreed with the periods predicted by the above equation.

Motility Assay

Flow chambers which allowed exchange of solutions for the motility assays had dimensions of 18 mm × 5 mm × ~75 μm and were made by placing a cover glass onto a microscope slide on which lay two lines of vacuum grease containing shards of #00 coverslip spacers (kindly supplied by Dr. D. Warshaw, University of Vermont, Burlington, VT). All solutions except some containing microtubules were made in Pipes buffer. The glass surfaces were precoated with ~2.5 mg/ml casein solution. A second solution containing kinesin (~10 nM) and 0.25 mg/ml casein was then introduced into the chamber. The solution following kinesin contained microtubules (total tubulin ~20-80 μg/ml) and 0.5 mM AMP-PNP. The AMP-PNP was added to bind the microtubules to the surface; any microtubules that were not on the surface could then be removed by the flow of the next solution thereby reducing the background fluorescence. The final solution introduced into the chamber was an anti-fade motility buffer: 0.285 M 2'-mercaptoethanol (βME), 40 mM D-glucose, 800 nM glucose oxidase, 160 nM catalase, 10 μM taxol, 2 mM ATP, and 2 mM $MgCl_2$ in Pipes buffer (adapted from Belmont et al., 1990). This same buffer was used for all the motility experiments. For low-density kinesin assays (performed only for the doublet-seeded microtubules), 1 nM kinesin (in a casein-containing buffer) was introduced into the chamber which gives a density of $<30\ \mu m^{-2}$ (see Howard et al., 1989, 1993 for calculations). Assays were done at room temperature.

Motility was observed by fluorescence microscopy using a Diastar microscope (Leica Inc., Deerfield, IL) equipped with a rhodamine fluorescence cluster. Images were detected with a silicon-intensified target camera (C2400-8, Hamamatsu Phototonic, Bridgewater, NJ; Bartels and Stout) and recorded with a ½-in video cassette recorder (either a Panasonic AG-6300 or a Mitsubishi HS-U55). Microtubules grown off doublets were also analyzed using dark-field microscopy using a 1.2–1.4 NA condenser (Carl Zeiss Oberkochen, Germany).

Velocity measurements were made using MEASURE hardware (M. Walsh Electronics, San Dimas, CA) and software kindly provided by Dr. S. Block (Rowland Institute, Cambridge, MA; described in Sheetz et al., 1986). The software was revised by Alan Hunt (University of Washington, Seattle, WA) to include regression analysis for determining the speed of microtubule movement. The digitized images were corrected numerically for field distortion in the camera.

Results

Structure of Microtubules under Electron Cryomicroscopy

To detect the predicted kinesin-induced rotation of microtubules summarized in Fig. 1, it was necessary to find assembly conditions for the in vitro polymerization of tubulin such that different microtubule preparations contained a majority of either 12-, 13-, or 14-protofilament microtubules.

Microtubules were polymerized under several different assembly conditions and were viewed by electron cryo-microscopy (Fig. 2). Each microtubule image consisted of two dark edges and a lighter central pattern containing zero to four striations. This central pattern is a moiré pattern caused by the superposition of the images of the protofilaments forming the "top" and "bottom" surfaces of the microtubule. The moiré patterns segregated into several distinct classes, and the lattice-rotation model permitted the assignment of a protofilament number between 10 and 16 to each of these classes (Wade et al., 1990*a*,*b*). For example, one class is characterized by either a lack of central striations or two parallel striations which are maintained over relatively large distances (>1 μm, Fig. 2, *13 protofilaments*). The interpretation of this pattern is that the protofilaments run parallel to the microtubule's long axis, as shown for the 13-protofilament A fiber of the axoneme (Amos and Klug, 1974). All the other classes correspond to microtubules with supertwisting protofilaments, and protofilament numbers other than 13. For example, the lattice-rotation model predicts that a microtubule which has a central moiré pattern with successive regions of one striation, no striations, and two striations (1-0-2) and with a repeat period of ~0.3 μm possesses 12 protofilaments (Fig. 2). Likewise, a microtubule with a 2-0-3 pattern has 14 protofilaments. A computer-generated moiré

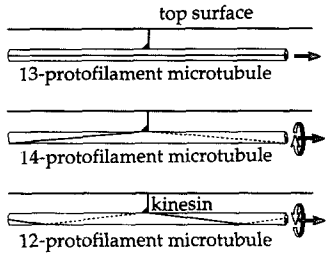

Figure 1. The effect of three types of protofilament lattices on movement. This cartoon depicts the three main kinds of microtubules of interest for testing the hypothesis that kinesin follows a single protofilament. In all cases the microtubules are shown moving to the right by a motor protein adsorbed to the top surface of a flow chamber. The 13 mer will not exhibit rotations since it has paraxial protofilaments. The 14 mer has a left-handed, supertwisted protofilament-lattice; if kinesin moves parallel to the protofilaments then the microtubule should rotate counterclockwise when looking in the direction of motion. The 12-mer has a right-handed supertwisted protofilament-lattice, and the rotation is predicted to be clockwise.

Published June 1, 1993

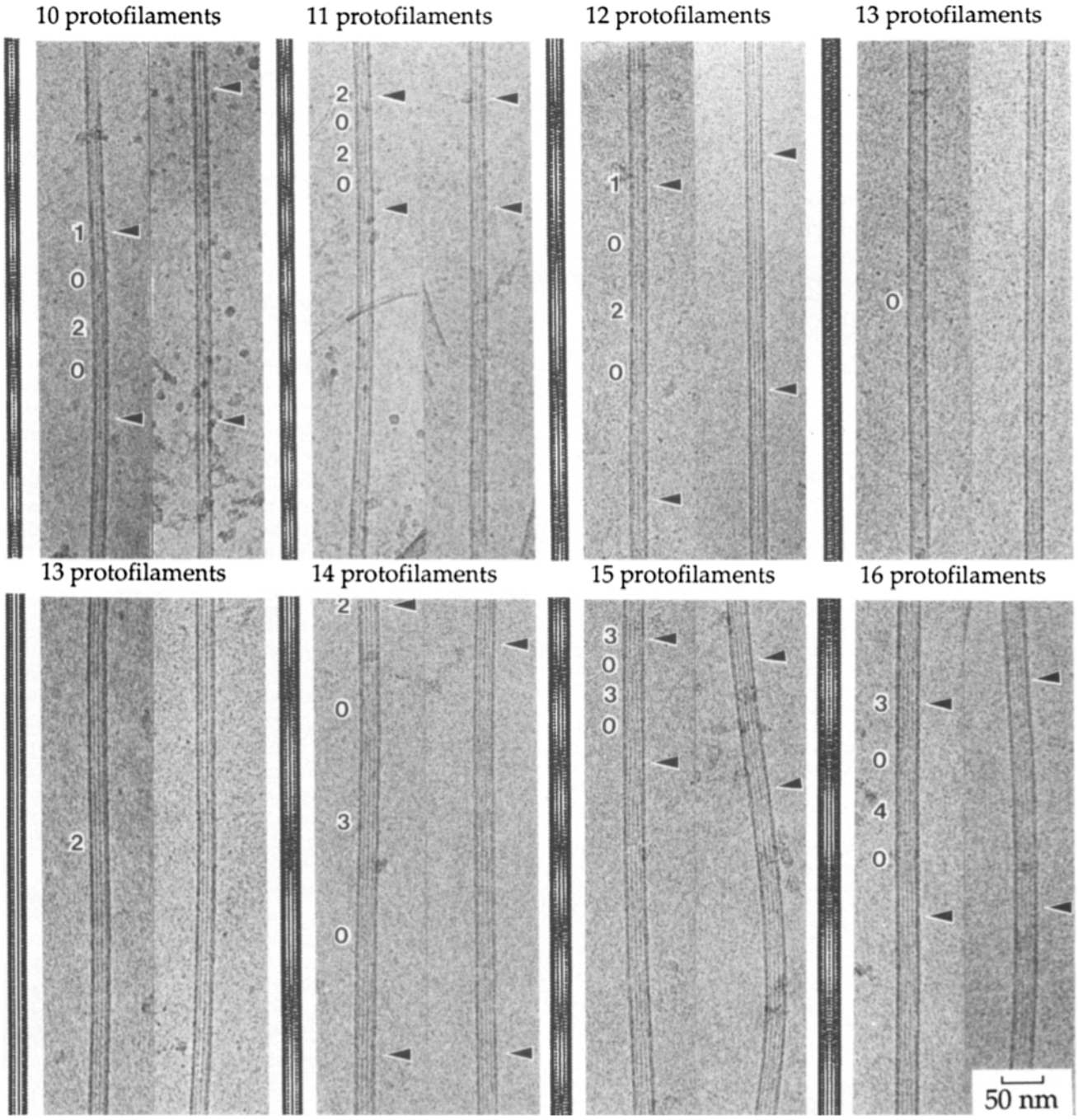

Figure 2. Electron cryo-microscopy and models of image projections of different microtubules. Representative examples of electron micrograph images of frozen hydrated microtubules with 10 to 16 protofilaments are shown. The moiré repeat distance is indicated by the arrows, and the numbers next to the microtubules indicate the number of striations in the central portion of the microtubule. The patterns are accentuated by viewing the page at a glancing angle. Next to each set of microtubules we also show a computer simulation of the moiré image structure predicted by the lattice–rotation model. Both the electron micrographs and the model microtubules are shown at the same magnification. Note the close agreement of the moiré patterns and repeat distance between the computer simulations and micrographs. The two examples of 13-protofilament microtubules show the two nonrepeating moiré patterns expected depending on the orientation of the microtubule on the grid.

pattern predicted by the lattice-rotation model is shown next to the examples from each class of images.

The assignment of a protofilament number to each image type was independently checked by plotting the moiré period against the diameter for microtubules grown under each of the several different assembly conditions (Fig. 3). Each microtubule could be unequivocally classified based on its diameter, moiré pattern, and moiré period. The mean di-

Published June 1, 1993

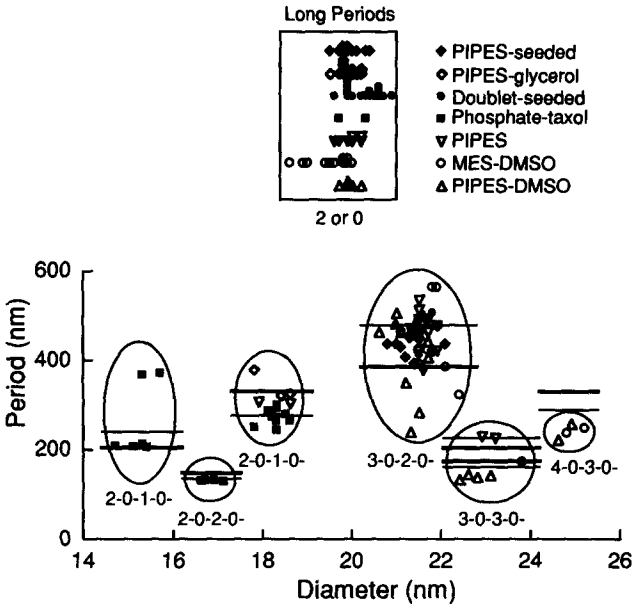

Figure 3. Moiré period vs. microtubule diameter. For the different assembly conditions we plotted the moiré period of the microtubules against the diameter. For 13 mers (2 or 0 pattern, see Fig. 2), which have no supertwist (or a very shallow supertwist) the repeat period is very long (>1.0 μm) and the histograms of diameters are displayed on the graph for comparison to the other microtubules. Microtubules with the same moiré pattern are enclosed by ellipses. But note that the diameter and repeat period could equally well have been used for the classification. It is evident that different assembly conditions lead to microtubules with the same microtubule surface lattice structure. Thick lines indicate the mean periods of the moiré patterns predicted by the lattice-rotation model. Thin lines indicate the predictions with the additional assumptions that 13 mers have a slight right handed supertwist of pitch 25 μm. The two pairs of lines associated with the 15 mers (3-0-3-0-) correspond to three-start (*upper pair*) and four-start (*lower pair*) lattices.

ameter associated with each microtubule class was found to differ from that of the other classes by an integral multiple of 1.7 nm, as expected if the microtubules in different classes have different protofilament numbers. If we identify the microtubules with a degenerate moiré pattern (a period >1 μm) as having 13 protofilaments (Amos and Klug, 1974; Wade et al., 1990*a*,*b*), the diameter of each microtubule can be used to unambiguously deduce its protofilament number. This assignment agreed always with that made on the basis of the structure of the moiré pattern predicted by the lattice-rotation model. Furthermore, with the exception of the 10 mers, the period of the moiré pattern of each microtubule class is in reasonable agreement with that predicted by the lattice-rotation model (bold horizontal lines in Fig. 3). Table I summarizes the distribution of protofilament numbers of microtubules grown under the various conditions.

The Majority of the Doublet-seeded Microtubules Did Not Rotate

It was necessary to grow 13 mers which were in some way marked so that rotation, if it occurred, would be detectable. The resolution of the light microscope is much too poor to resolve the surface lattice of a microtubule and it is not possible to detect the rotation of a straight, unmarked microtubule as it moves across the surface. The way that we produced marked 13 mers was to polymerize microtubules off axoneme doublets. Doublets consist of a complete A fiber microtubule which has 13 protofilaments and an incomplete B fiber which has 10 protofilaments (Amos and Klug, 1974). In vitro, growth off doublets extends preferentially from the A fiber when free tubulin is less than 1 mg/ml (Scheele et al., 1982). As expected from previous results (Scheele et al., 1982), 90% of these microtubules had 13 protofilaments (Table I) based on their diameters and their paraxial protofilaments. The great preponderance of 13 mers assembled under these conditions makes us fairly confident that much of the growth occurred off the doublet seeds (compare with 78% 13 mers in MES-glycerol and 54% 13 mers in MES-DMSO in Table I). We were therefore surprised that we never saw doublets under the electron microscope. One possible explanation is that most of the doublets from the doublet-seeded microtubules were lost during the additional centrifugation step necessary for concentrating the microtubules for EM.

For the in vitro motility assays, short segments (<5 μm) of curved doublets were incubated in rhodamine-labeled tubulin to produce tripartite microtubules: they each had a straight, relatively short, fluorescent segment corresponding to the slow-growing or minus end; a non-fluorescent curved segment corresponding to the curved doublet; and a straight, relatively long, fluorescent segment corresponding to the fast-growing or plus end. An example of such a microtubule under the fluorescent microscope is shown in Fig. 4: the shorter minus end (marked with an arrow) is pointing down into the solution and out of focus; at a later time (24 s) the minus end of the same microtubule is clearly visible after it

Table I. Distribution of Protofilament Number in Various Assembly Conditions

	Percentage of microtubules in each protofilament class							
	10	11	12	13	14	15	16	Total
Doublet seeded	0	0	1	**90**	9	0	0	250
PO_4-taxol	2	9	**77**	11	2	0	0	297
Pipes-glycerol	0	0	6	39	**53**	2	0	310
Pipes seeded	0	0	5	42	**52**	1	0	142
Pipes-DMSO	0	0	0	14	**72**	11	3	65
Pipes	0	0	4	32	**61**	3	0	248
MES-glycerol	0	0	4	**78**	15	4	0	27
MES-DMSO	0	0	2	**54**	38	2	4	68

Published June 1, 1993

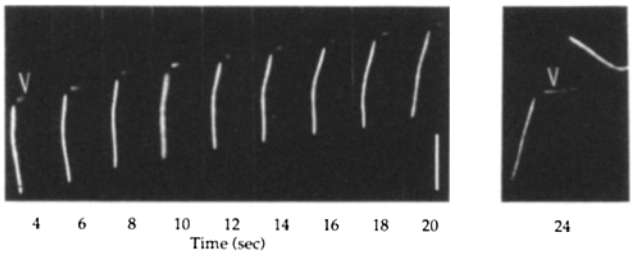

Figure 4. Motion of a 13-protofilament microtubule. A doublet-seeded microtubule moving across a kinesin-coated glass surface and viewed under fluorescence microscopy did not rotate. Shown here are 16 s of movement during which the fluorescent minus end remained out of focus (directed off the surface into the solution) because the microtubule was not rotating. The image at 10 s is focused slightly below the surface to better view the minus end. The right most image is at a later time (24 s) when the minus end had become attached to the surface. Bar, 10 μm.

became attached to the surface. By switching the microscope optics to darkfield, we confirmed that the middle segment was actually brighter than the two flanking segments, consistent with the greater expected mass of the doublet microtubule. Provided that the short minus end is angled away from the surface and unable to interact with kinesin, these doublet-seeded microtubules serve as good markers for observing rotations. This microtubule moved such that its shorter, leading, minus-end was not attached to the surface as it moved for 42 s over a distance of ~40 μm. Over this time, no rotations were observed. If the path followed by kinesin along this microtubule were actually part of a very long-pitch helix, then the pitch must be in excess of ~80 μm. Another 126 microtubules showed no detectable rotation over distances from 10 to 65 μm.

Two of the doublet-seeded microtubules actually did rotate: this shows that the assay was sensitive to such rotations. One of these two microtubules underwent five rotations with an average pitch -5.4 μm, where the minus sign indicates that the handedness of the rotation was counterclockwise when looking in the direction of motion toward the microtubule's minus (leading) end. The other microtubule made a one-half rotation when only the last 10 μm of its plus end was attached to the surface. We believe that in these two microtubules, the protofilament number probably switched from 13 to 14, as described by Chrétien et al. (1992), and that the rotations therefore reflect the path taken along the supertwisted 14-protofilament lattice (see below).

Kinesin Follows the Protofilament Axis of 13 Mers with High Fidelity

The fidelity of movement of kinesin with respect to the protofilament lattice must be very high. Suppose kinesin occasionally undergoes transitions from one protofilament to another as it steps along the lattice; what is an upper bound on the probability of such transitions? If kinesin steps from dimer to dimer, a distance of 8.2 nm, the probability of moving say to the protofilament to the right is 0.01, and then we expect the microtubule to rotate with a pitch of 13 × 8.2 nm/0.01 = 10.7 μm (if the distance between sites were 4.1 nm, the rotation would be even more pronounced). Because this distance is much shorter than the measured lower bound of the rotational pitch, we tentatively conclude that the probability of making such a transition must be <0.01. However, it is likely that in the above assay with the doublet-seeded microtubules, several kinesin molecules were moving each microtubule. It is then possible that the presence of many motors had a steadying effect by sterically preventing any one of the motors from switching protofilaments. Therefore, we repeated the experiments at approximately tenfold lower kinesin density on the surface: at this density we expect on average only one to two motors to be moving a microtubule at any one time (Howard et al., 1989; Block et al., 1990). In many cases, a microtubule would pivot about a single point on the surface indicating that the forward motion was likely due to a single kinesin molecule located at this point. We observed eight such pivoting microtubules move through distances of 2–8 μm without noticeable rotation. In the case of the microtubule which moved for 8 μm, the rotation was certainly <90°. This implies that if kinesin has a bias to move circumferentially around the microtubule then the pitch of this rotation is greater than 32 μm and so the probability of making such a transition is much less than 0.01 per step in the longitudinal direction.

There is another way in which the motion with respect to the protofilament axis could be unreliable: kinesin may randomly switch from one protofilament to another in an unbiased manner. If at each step, kinesin has a probability equal to p of making a transition to the neighboring protofilament at one side, a probability equal to p of making a transition to the other side, and a probability equal to 1–2 p of remaining on the same protofilament, then we expect the microtubule to undergo a random rotatory motion (with statistics given by the trinomial distribution) such that after N steps the microtubule is likely to have rotated through 2π ($\sqrt{2Np}/13$) radians. For example, if $p = 0.01$ then after 1,000 steps the microtubule is likely to have rotated through ~120°. Such a large rotation was never observed even though it would have been easily noticed. By applying a statistical analysis to the motion of the eight microtubules that pivoted about a single point, we placed an upper bound on the probability of switching to a different protofilament: if the distance between consecutive binding sites is 8 nm, then at the 97% confidence level $P < 0.01$; if this distance is 4 nm, then the confidence level that $P < 0.01$ increases to 99.97%. If the switching has both biased and random components, then probability of switching either way must be <0.02.

Tail Structures Serve As Markers for Rotation

To detect the predicted rotation of 12- and 14-protofilament microtubules, we needed a marker for rotation. Fortunately, we found that under certain assembly conditions, a small percentage of the microtubules had a short, coiled structure at one or the other end. Figs. 5 *a* and 6 *a* show two microtubules with such coiled structures at their plus ends. We call these structures "tails" because they were found mostly at the plus (or trailing) ends of microtubules (89%; 65 out of 73).

We believe that the tails are probably incomplete microtubules containing fewer than eight protofilaments that would appear as a C shape in cross-section rather than a closed O. The following observations support this belief. First, under

Published June 1, 1993

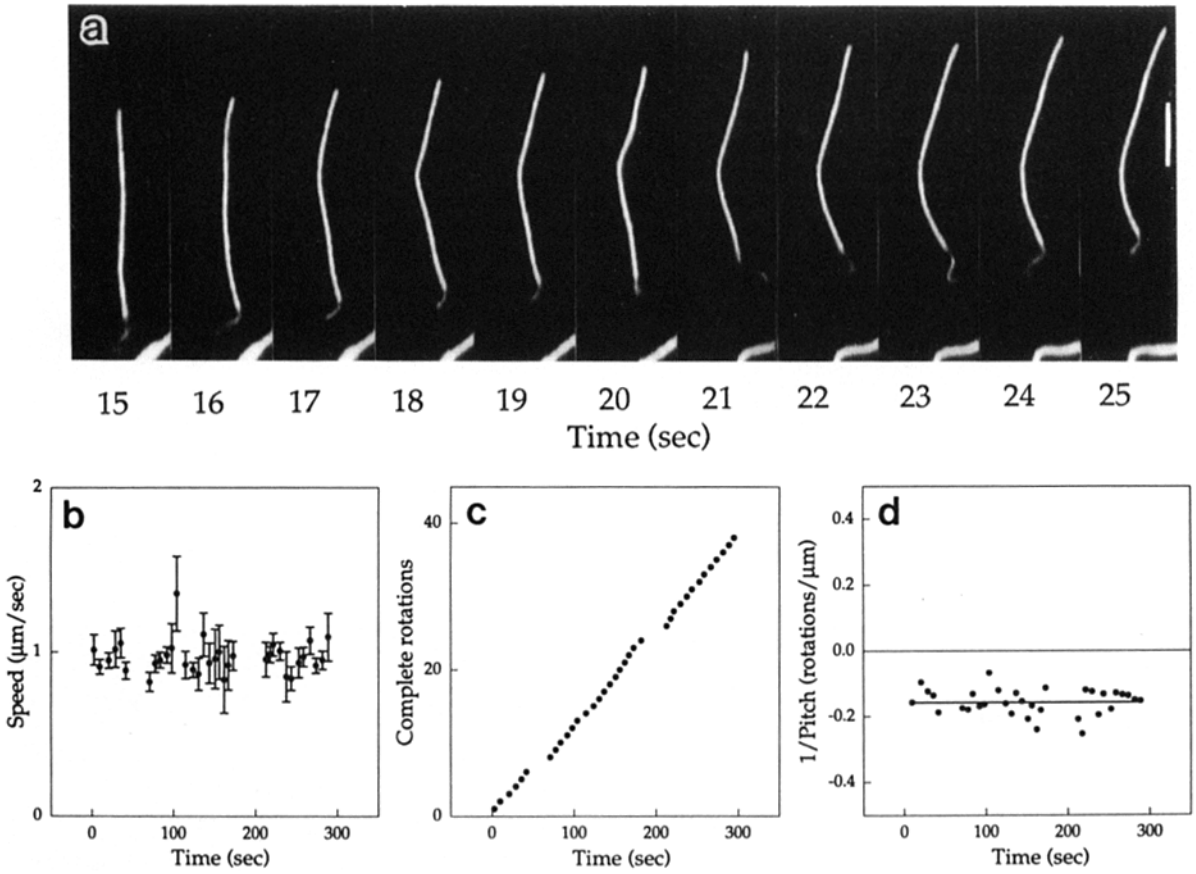

Figure 5. Motion of 14-protofilament microtubules. (*a*) A moving microtubule with a long tail underwent a complete counterclockwise rotation: the tail went out of focus to the left and came back into focus on the right. The handedness is evidently counterclockwise because the microtubule was moving across the top surface of the flow cell which means that an out-of-focus object is in the subjacent solution. (*b*) The speed of a different microtubule over a period of 300 s. The lacunae correspond to times when the field of view was moved to follow the microtubule. (*c*) The cumulative complete rotations for the same microtubule as in *b* is plotted against time. (*d*) The inverse of the rotational pitch in units of μm^{-1} (the angular velocity in units of complete rotations per second divided by the translational velocity in units of microns per second) is plotted against time. The horizontal line corresponds to the average inverse pitch of $-0.162\ \mu m^{-1} = -(6.16\ \mu m)^{-1}$. Bar, 6 μm.

epifluorescence, the tails were dimmer than the rest of the straight microtubule—we guess that they contain fewer than eight protofilaments since it has been observed that eight protofilaments can form a closed microtubule. Second, because they were moved continuously by kinesin, the tails are probably composed of protofilaments. Third, the presence of taxol, DMSO, and glycerol, all of which have been shown to stabilize incomplete microtubules (Schiff et al., 1979; Kamimura and Mandelkow, 1992; Müller et al., 1990), made tails more abundant. Our tails most likely have a similar structure to the unclosed "C-tubules" recently shown by Kamimura and Mandelkow (1992) to be moved by kinesin in vitro. Fourth, the hypothesis that the tails are incomplete microtubules explains in a very natural way why they are coiled. The reason why any microtubule is straight is that it is closed: in this way any tendency of the protofilaments to deviate from linearity is canceled as one integrates around the microtubule's circumference. Because individual protofilaments at the ends of microtubules tend to coil outward (Mandelkow et al., 1991) it is expected that an unclosed microtubule will also be coiled. Finally, the shape of the tails was not related to the protofilament supertwist: of 73 tails, only 38 were long enough for us to determine their handedness, and all 38 with long tails were right handed. These 38 examples included microtubules which rotated clockwise, did not rotate, and which rotated counterclockwise, corresponding respectively to 12-, 13-, and 14-protofilament microtubules (see below). The handedness of a tail is perhaps most apparent in the 7th frame of Fig. 5 *a* (19 s) where the tail goes out of focus down into the solution in a right-handed manner. Furthermore the pitch of the tail helix, 2.6 $\pm$ 1.1 μm (mean $\pm$ sd; $n = 13$), was not equal to the pitch of any of the most common supertwist pitches. The pitch and handedness of the "tails" was close to that of the "hyperflexible regions" described by Dye et al. (1992), indicating that the two structures are probably similar. Irrespective of their structure, these tails served as good markers for observing microtubule rotation.

The Majority of the Microtubules Grown in Pipes Buffer Rotated Counterclockwise

Most of the microtubules initially seeded in Pipes in the pres-

Published June 1, 1993

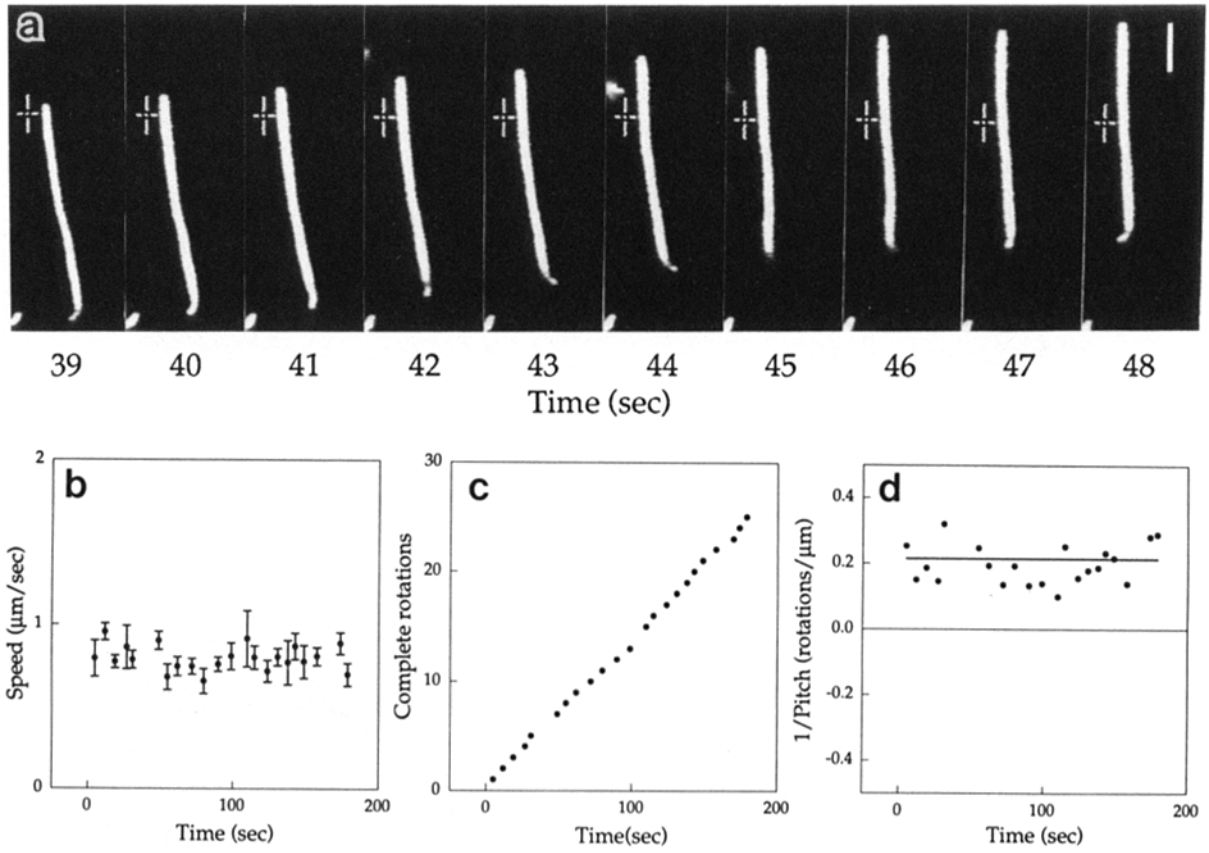

Figure 6. Motion of 12-protofilament microtubules. (*a*) A microtubule takes a complete clockwise rotation: the tail approached the surface from the left and went out of focus on the right. (*b–d*) The speed, cumulative rotations, and pitch of another microtubule. The horizontal line in *d* corresponds to a pitch of +4.68 μm. Bar, 4 μm.

ence of glycerol and then grown further in the same buffer but without glycerol contained 14 protofilaments as determined from their moiré patterns and diameters (52%, Table I). Of the remaining microtubules, most had 13 protofilaments (42%). The average period of the moiré pattern of the Pipes-seeded 14 mers was 0.445 ± 0.029 μm (mean ± SD, n = 9), in good agreement with the average period of the moiré pattern of 14 mers grown under all conditions (0.447 ± 0.059 μm, mean ± SD, n = 60). The corresponding supertwist pitch is predicted to equal the product of this period and the number of protofilaments: this corresponds to 6.2 ± 0.4 μm (mean ± SD, n = 9) for these 14 mers (Table II).

The movement of Pipes-seeded microtubules across kinesin-coated surfaces was observed. Of 29 microtubules which had tails, 12 rotated counterclockwise as they moved across the surface, seven clearly did not rotate, seven probably did not rotate, and three could not be classified. No microtubules were observed to rotate clockwise.

Fig. 5 *a* shows a complete counterclockwise rotation of a microtubule moving across the top surface of a flow cell: in the first frame the tail is in focus at the surface and points towards the left; in the next few frames it moves downwards into the solution and partly out of focus; at 21 seconds the tail begins to come back into focus, this time pointing towards the right. Note that the rotation of the tail is impeded at 22 s as the tail is coming back to the surface from the solution prior to completing the rotation. The entire rotation took about 7.6 s during which the microtubule moved 6.8 μm. The motion of a different microtubule is analyzed in Figs. 5, *b–d*: this microtubule was more suitable for pitch measurements because it had a smaller tail which did not get caught as often by motors on the surface. The microtubule moved at an average speed of ~1 μm/s (Fig. 5 *b*) for ~5 min (before

Table II. Summary of Conclusions: the Supertwist Pitches Correspond to the Rotational Pitches

	Protofilament number		
	12 mean ± SD (μm) (n)	13 mean ± SD (μm) (n)	14 mean ± SD (μm) (n)
Doublet seeded	–	long*	6.1 ± 0.8 (4)
PO_4-taxol	3.4 ± 0.2 (13)	long*	–
Pipes seeded	–	long*	6.2 ± 0.4 (9)
Lattice rotation model	+4.0	∞	−5.5
Modified model	+3.4	+24.8	−6.8
Rotation	+3.7 ± 0.9 (24)	not seen	−5.9 ± 1.1 (13)

* In certain conditions, some supertwist pitches were as short as 25 μm whereas others were at least as long as 65 μm.

Published June 1, 1993

it became too photobleached) and underwent 36 rotations (Fig. 5 *c*), with an average rotational pitch of −6.16 μm (Fig. 5 *d*) where the negative sign indicates a counterclockwise rotation.

The average pitch of seven microtubules which rotated was −8.0 ± 1.8 μm (mean ± SD; 125 rotations). This value probably overestimates the mean of the absolute pitch: sometimes the tail, especially if it was long, was attached to the surface along its whole length. During these times complete rotations may have occurred. A failure to detect such rotations would then lead to an apparent doubling of the pitch as was sometimes observed. To obtain a better estimate of the rotational pitch, we restricted our measurements to microtubules with shorter tails and to times when the tails were free from attachment to the surface: 13 such rotations by five microtubules gave a pitch of −5.9 ± 1.1 μm (mean ± SD).

The Majority of the Microtubules Grown in Phosphate Buffer with Taxol Rotated Clockwise

Most of the microtubules polymerized in the presence of taxol in phosphate buffer (Andreu et al., 1992) contained 12 protofilaments (78%, Table I) as determined from their moiré patterns and diameters. 11% had 13 protofilaments. The average period of the moiré pattern of these 12 mers was 0.283 ± 0.016 μm (mean ± SD, n = 13), similar to the average period of the moiré pattern of 12 mers grown under all conditions (0.287 ± 0.029 μm; mean ± SD, n = 35). The corresponding supertwist pitch of these 12 mers is predicted to be 3.4 ± 0.2 μm (mean ± SD, n = 13; Table II).

Of nine microtubules which had tails, seven rotated clockwise when looking toward the minus end while two showed no evidence of rotation. Fig. 6 *a* shows a microtubule making one clockwise turn when looking at the minus end. This is clearly seen because the tail went into the solution (out of focus) from the right between 43 and 45 s (Fig. 6 *a*). Analysis of the speed (Fig. 6 *b*) and cumulative number of rotations (Fig. 6 *c*) for another microtubule gave an average rotational pitch of +4.68 μm (Fig. 6 *d*). For three microtubules followed over long distances, the average pitch of rotation was +5.4 ± 0.5 μm (mean ± SD, 27 rotations). As in the case of 14 mers, we believe that these measurements again overestimate the true rotational pitch: it is possible that some rotations were missed due to the interaction of the tail with the surface. For example, the pitches of two turns when the tail was clearly detached from the surface were +3 and +3.8 μm. Because the number of examples of such unobstructed motion was small in the case of taxol, we measured the rotational pitch during only that half of the rotation when the tail was moving through the solution: the pitch was +3.7 ± 0.9 μm (mean ± SD, 24 half-rotations).

Discussion

Kinesin Follows a Path Parallel to the Protofilaments

The main conclusion of this work is that the path kinesin follows along the surface lattice of a microtubule is parallel to the axis defined by the protofilaments. The support for this conclusion comes from the following observations. Electron cryo-microscopy showed that the majority (90%) of doublet-seeded microtubules had 13 protofilaments which ran parallel (or nearly parallel) to the microtubules long axes. Also, the majority (98%) of these doublet-seeded microtubules did not noticeably rotate as they moved across a kinesin-coated surface. We tentatively conclude that the lack of rotation was due to kinesin following a path parallel to the paraxial protofilaments. But it is possible that rotations were blocked or somehow not detected. For this reason we observed the motion of microtubules with supertwisted protofilaments. Approximately half (52%) of the Pipes-seeded microtubules had 14 protofilaments and a corresponding supertwist pitch of 6.2 ± 0.4 μm (mean ± SD, n = 9) as measured by electron cryo-microscopy. In the motility assay 12/26 of the Pipes-seeded microtubules rotated with a pitch of ~6–8 μm. The simplest explanation is that the rotating microtubules are the 14 mers and that kinesin is following the protofilament axis. Similarly, the majority of the taxol-polymerized microtubules (77%) had 12 protofilaments with corresponding supertwist pitch of 3.4 ± 0.2 μm (mean ± SD, n = 13), and the majority of the microtubules grown under the same conditions (7/9) rotated with a pitch of 3–4 μm. Again this is consistent with kinesin following the supertwisting, protofilament axis. Finally, the handedness of the rotations of the Pipes-seeded and taxol-polymerized microtubules are of opposite sign and in both cases the handedness agrees with the handedness of the supertwist expected for 14- and 12-protofilament microtubules, respectively (see Introduction). Taken together these observations strongly suggest that kinesin follows the protofilament axis.

The Protofilament Supertwist and the Lattice-Rotation Model

Our conclusion that kinesin follows the protofilament axis rests on the assumption that the microtubules used for the cryo-electron microscopic assays and the microtubules used for the corresponding motility assays had the same structure: that (*a*) the proportion of microtubules in each protofilament class was the same for both assays; and (*b*) microtubules with the same protofilament number had the same supertwist. The arguments that support these assumptions are as follows: (*a*) The microtubules were grown in virtually identical conditions for both assays. It was only after taxol stabilization that the buffer was changed for the motility assays (which were all done in identical buffers). We think it is unlikely that changing the buffer in this way altered the distribution of microtubules in the various protofilament classes because this would have entailed depolymerization and repolymerization; but taxol blocked depolymerization. (*b*) The cryo-electron microscopy shows quite clearly that the supertwist pitch depends only on the number of protofilaments and not on the particular buffer that bathed the microtubule. For example microtubules which were deduced to have 14 protofilaments from their diameter had the same moiré periods (up to the accuracy of these micrographs) irrespective of whether they were bathed in Pipes, MES, phosphate–taxol, etc. Note that these are very different conditions: for example the ionic strength ranges from ~40 mM through to ~160 mM. Thus, neither the buffering agent nor taxol profoundly changes the supertwist of a given microtubule. None-the-less there were other differences, such as the βME, ATP, and antioxidant enzymes that were added only to the motility buffers. While we cannot absolutely exclude

Published June 1, 1993

the possibility that they have drastic effects on the supertwist we have no indication that they do. In fact, it is difficult to find a self-consistent explanation for the correlation between the measured rotational pitches and the supertwist pitches if the supertwists were drastically changed by, for example, βME.

Our structural data significantly bolster the Wade-Chrétien lattice–rotation model. Electron micrographs of microtubules grown under several assembly conditions, revealed microtubules with protofilament numbers ranging from 10 to 16 protofilaments. In all but two cases (two of the 10 mers), the supertwist period was close to that predicted by the lattice–rotation model, provided that the 10 mers have a two-start monomer helix and the 16 mers have a four-start monomer helix. As pointed out by Chrétien and Wade (1991) the 10 mer is expected to be a two-start helix and the 16 mer is expected to be a four-start helix in order to minimize the rotation of the surface lattice.

There are small but significant deviations of the measured supertwist pitch from the lattice–rotation model (see Fig. 2 and Table II). The deviations are also systematic: the microtubules which are predicted to have a right-handed supertwist have a measured moiré period smaller than predicted, while those predicted to have a left-handed supertwist have longer measured moiré periods. These observations are consistent with the assumption that the 13 mers viewed under the electron microscope have a slight right-handed supertwist with pitch of +25 μm and moiré period of 1.9 μm (Table II, and the faint horizontal lines in Fig. 3). Indeed, several microtubules which could be followed in the electron micrographs over long distances appeared to have periods of this magnitude, though other microtubules definitely had periods >3 μm corresponding to pitches >39 μm. Thus, the structural observations are more consistent with 13 mers having a small, variable, but significantly right-handed supertwist. On the other hand, the motility data indicates that the 13-protofilament supertwist is longer than 25 μm, and that the 12 and 14 mers have supertwist pitches more nearly equal to those predicted by the lattice–rotation model than those measured from the electron micrographs. One possible explanation is that the procedure for the preparation of microtubules for electron cryo-microscopy may introduce a small handedness preference.

Comparison to Earlier Work

Gelles et al. (1988) also concluded that kinesin follows the protofilament axis. They tracked the movement of kinesin-coated plastic beads along stationary microtubules using high-precision video analysis: the beads did not show the large lateral fluctuations expected by the authors to signify switching of the beads to different protofilaments. By taking a completely different experimental approach, our results provide strong additional evidence that their original conclusion is correct. Furthermore, we have extended the observations to low densities in order to show that even a single motor can follow the protofilament axis with high fidelity.

The fact that kinesin can rotate some microtubules implies that kinesin is capable of generating torque. But the fact that kinesin does not always produce rotations, implies that torque generation is as much a property of the filament as of the motor. Torque generation has been described for two other microtubule-based motors: 14S dynein (Vale and Toyoshima, 1988) and the kinesin-related protein *ncd* (Walker et al., 1990) both rotate doublet-seeded microtubules. The measured rotational pitches were +0.54 ± 0.13 μm and +0.3 ± 0.12 μm, respectively, much shorter than the supertwist pitches (here the sign refers to the right-handed helical path on the microtubules' surfaces that the motors presumably follow). The structural basis for the rotation by 14S dynein and *ncd* is a mystery: the motors do not follow the protofilament axis, nor do they follow any of the three major helices of a microtubule because the three-start monomer helix, and the five- and eight-start dimer helices of 13 mers have much shorter pitches of −12.3, +41, and −65.6 nm, respectively (Amos and Klug, 1974) and two of them are of the wrong handedness. It is conceivable that they follow one of the shallower monomer helices which have the correct handedness such as the 23 start (pitch = +94 nm), the 36 start (+148 nm), or the 49 start (+201 nm). The 36-start helix would require a distance between consecutive motor-binding sites across the microtubule lattice of ~12.5 nm.

We have been careful in stating our conclusion as "kinesin follows a path parallel to the protofilament axis" rather than "kinesin moves along a single protofilament." This is because our data cannot distinguish whether kinesin binds exclusively on one protofilament or binds in the groove between adjacent protofilaments. On the other hand, Kamimura and Mandelkow (1992) suggested that kinesin can move zinc-induced sheets of tubulin. Neighboring protofilaments of the sheets alternate in polarity and surface orientation. Because this implies abnormal lateral association between protofilaments, their result suggests that the binding site for kinesin lies exclusively on the protofilament. Their experiments may be quite complementary to our own because they cannot tell whether kinesin moves exclusively along one protofilament or whether kinesin jumps from one properly oriented protofilament to another. Taken together, our and their experiments would indicate that kinesin moves along a single protofilament.

What is the distance between consecutive kinesin binding sites on the surface of the microtubule? Since neither tubulin monomer contains repeated sequences of amino acids, it is unlikely that there is more than one kinesin-binding site per monomer. Therefore, the inference from our finding that kinesin moves, with such high fidelity, parallel to the protofilaments, rather than switching between protofilaments, is that the distance between consecutive microtubule binding sites must be an integral multiple of 4.1 nm, the spacing between the monomers along the protofilament, or 8.2 nm the interdimer spacing.

We thank Drs. L. Amos and R. Wade for initial discussions, and Mr. Sung Baek who first saw the tails. We thank Drs. P. Detwiler, A. M. Gordon, A. J. Hudspeth, and T. Wensel, and F. Gittes and A. Hunt for helpful comments on an earlier manuscript.

This work was supported by the National Institutes of Health (AR40593 (J. Howard), AR39155 (R. A. Milligan), 5T32NS07097 (S. Ray) and a Feasibility Study Grant from the Alzheimer's Disease Research Center at University of Washington to J. Howard), the Washington Affiliate of the American Heart Association (E. Meyhöfer), and the Alfred P. Sloan Foundation (J. Howard). J. Howard is a Pew Scholar in the Biomedical Sciences. R. A. Milligan is an Established Investigator of the American Heart Association.

Received for publication 15 December 1992 and in revised form 4 March 1993.

Published June 1, 1993

References

Adrian, M., J. Dubochet, J. Lepault, and A. W. McDowall. 1984. Cryo-electron microscopy of viruses. *Nature (Lond.)*. 308:32–36.

Amos, L. A., and A. Klug. 1974. Arrangement of subunits in flagellar microtubules. *J. Cell. Sci.* 14:523–549.

Andreu, J. M., J. Bordas, J. F. Diaz, J. García de Ancos, R. Gil, F. G. Medrano, E. Nogales, E. Pantos, and E. Towns-Andrews. 1992. Low resolution structure of microtubules in solution. Synchrotron X-ray scattering and electron microscopy of taxol-induced microtubules assembled from purified tubulin in comparison with glycerol- and MAP-induced microtubules. *J. Mol. Biol.* 226:169–184.

Belmont, L. D., A. A. Hyman, K. E. Sawin, and T. J. Mitchison. 1990. Real-time visualization of cell cycle-dependent changes in microtubule dynamics in cytoplasmic extracts. *Cell.* 62:579–589.

Block, S. M., L. S. Goldstein, and B. J. Schnapp. 1990. Bead movement by single kinesin molecules studied with optical tweezers. *Nature (Lond.)*. 348:348–352.

Böhm, K. J., W. Vater, P. Steinmetzer, and E. Unger. 1990. Effect of sodium chloride on the structure of tubulin assemblies. *Acta. Histochem. Suppl.* 39:365–371.

Bradford, M. M. 1976. A rapid and sensitive method for the quantitation of microgram quantities of protein utilizing the principle of protein-dye binding. *Anal. Biochem.* 72:248–254.

Chrétien, D., and R. H. Wade. 1991. New data on the microtubule surface lattice (and see erratum, 1991. *Biol. Cell.* 72:284). *Biol. Cell.* 71:161–174.

Chrétien, D., F. Metoz, F. Verde, E. Karsenti, and R. H. Wade. 1992. Lattice defects in microtubules: protofilament numbers vary within individual microtubules. *J. Cell Biol.* 117:1031–1040.

Dye, R. B., P. F. Flicker, D. Y. Lien, and R. C. Williams, Jr. 1992. End-stabilized microtubules observed in vitro: stability, subunit interchange, and breakage. *Cell Motil. Cytoskeleton.* 21:171–186.

Gelles, J., B. J. Schnapp, and M. P. Sheetz. 1988. Tracking kinesin-driven movements with nanometre-scale precision. *Nature (Lond.)*. 331:450–453.

Gibbons, B. H. 1982. Reactivation of sperm flagella: properties of microtubules-mediated motility. *Methods Cell Biol.* 25:253–271.

Howard, J., A. J. Hudspeth, and R. D. Vale. 1989. Movement of microtubules by single kinesin molecules. *Nature (Lond.)*. 342:154–158.

Howard, J., A. J. Hunt, and S. Baek. 1993. Assay of microtubule movement driven by single kinesin molecules. *Methods Cell Biol.* 37: In press.

Hyman, A., D. Drechsel, D. Kellogg, S. Salser, K. Sawin, P. Steffen, L. Wordeman, and T. Mitchison. 1991. Preparation of modified tubulins. *Methods Enzymol.* 196:478–485.

Kamimura, S. and E. Mandelkow. 1992. Tubulin protofilaments and kinesin-dependent motility. *J. Cell Biol.* 118:865–875.

Kikuchi, T., T. Takasaka, A. Tonosaki, Y. Katori, and H. Shinkawa. 1991. Microtubules of guinea pig cochlear epithelial cells. *Acta Otolaryngol. (Stockholm).* 111:286–290.

Langford, G. M. 1980. Arrangement of subunits in microtubules with 14 protofilaments. *J. Cell Biol.* 87:521–526.

Mandelkow, E., and E.-M. Mandelkow. 1990. Microtubular structure and tubulin polymerization. *Curr. Opin. Cell Biol.* 2:3–9.

Mandelkow, E.-M., E. Mandelkow, and R. Milligan. 1991. Microtubule dynamics and microtubule caps: a time-resolved cryo-electron microscopy study. *J. Cell Biol.* 114:977–991.

Milligan, R. A., A. Brisson, and P. N. T. Unwin. 1984. Molecular structure determination of crystalline specimens in frozen aqueous solutions. *Ultramicroscopy.* 13:1–10.

Müller, H., K. J. Böhm, W. Vater, and E. Unger. 1990. Structural changes within mixed populations of microtubules and protofilament ribbons caused by dilution and cold incubation. *Acta. Histochem. Suppl.* 39:373–378.

Scheele, R. B., L. G. Bergen, and G. G. Borisy. 1982. Control of the structural fidelity of microtubules by initiation sites. *J. Mol. Biol.* 154:485–500.

Scheetz, M. F., S. M. Block, and J. A. Spudich. 1986. Myosin movement in vitro: a quantitative assay using oriented actin cables from Nitella. *Methods Enzymol.* 134: 531–544.

Schiff, P. B., J. Fant, and S. B. Horwitz. 1979. Promotion of microtubule assembly in vitro by taxol. *Nature (Lond.)*. 277:665–667.

Vale, R. D., and Y. Y. Toyoshima. 1988. Rotation and translocation of microtubules in vitro induced by dyneins from Tetrahymena cilia. *Cell.* 52:459–469.

Wade, R. H., D. Chrétien, and D. Job. 1990*a*. Characterization of microtubule protofilament numbers. How does the surface lattice accommodate? *J. Mol. Biol.* 212:775–786.

Wade, R. H., D. Chrétien, and E. Pantos. 1990*b*. Concerning the surface lattice of microtubules. *In* Electron Crystallography of Organic Molecules. J. R. Fryer and D. L. Dorset, editors. Kluwer, The Netherlands. 317–325.

Wagner, M. C., K. K. Pfister, S. T. Brady, and G. S. Bloom. 1991. Purification of kinesin from bovine brain and assay of microtubule-stimulated ATPase activity. *Methods Enzymol.* 196:157–175.

Walker, R. A., E. D. Salmon, and S. A. Endow. 1990. The Drosophila claret segregation protein is a minus-end directed motor molecule. *Nature (Lond.)*. 347:780–782.

Weingarten, M. D., M. M. Suter, D. R. Littman, and M. W. Kirschner. 1974. Properties of the depolymerization products of microtubules from mammalian brain. *Biochemistry.* 13:5529–5537.